

¹⁸F-FDG PET SUVmax as an indicator of histopathologic response after neoadjuvant chemotherapy in extremity osteosarcoma

Chang-Bae Kong · Byung Hyun Byun · Ilhan Lim ·
Chang Woon Choi · Sang Moo Lim · Won Seok Song ·
Wan Hyeong Cho · Dae-Geun Jeon · Jae-Soo Koh ·
Ji Young Yoo · Soo-Yong Lee

Received: 11 September 2012 / Accepted: 4 January 2013 / Published online: 30 January 2013
© Springer-Verlag Berlin Heidelberg 2013

Abstract

Purpose This study evaluated the usefulness of the maximum standardized uptake value (SUVmax) as a measure of histologic response to neoadjuvant chemotherapy in patients with extremity osteosarcoma. The correlation between [¹⁸F] FDG PET SUVmax values and histologic response to pre-operative chemotherapy was also assessed prospectively using PET/MRI.

Methods A total of 26 consecutive patients with high-grade osteosarcoma were prospectively enrolled. All patients underwent parallel PET and MRI scans before and after neoadjuvant chemotherapy. Using the PET and MRI images and pathologic mapping, we assessed the percentage necrosis by histology at the highest metabolic activity point in the tumors. This was defined as the minimum histologic response. The predictive values of SUVmax before (SUV1) and after (SUV2) chemotherapy and the SUV change ratio were

determined. Correlations were also investigated among SUV2, minimum histologic response and histologic response. **Results** Histologically, 13 patients were classified as good responders and 13 as poor responders. Patients with an SUV2 of >5 showed a poor histologic response. A significant correlation was found between SUV2 and histologic response (Spearman's rho -0.642; $P < 0.001$), and SUV2 and histologic response were both found to be significantly correlated with minimum histologic response (Spearman's rho -0.515 and 0.911; $P = 0.007$ and $P < 0.001$, respectively).

Conclusion A SUVmax of more than 5 after neoadjuvant chemotherapy identified the majority of histologic nonresponders (sensitivity 61.3 %, PPV 88.9 %). Tumor necrosis at the point of maximum metabolic activity was found to be significantly correlated with the histologic response of entire resected specimen.

Keywords Osteosarcoma · FDG PET · SUVmax · Histologic response

C.-B. Kong · W. S. Song · W. H. Cho · D.-G. Jeon · S.-Y. Lee
Department of Orthopedic Surgery, Korea Cancer
Center Hospital, Seoul, South Korea

B. H. Byun · I. Lim · C. W. Choi · S. M. Lim (✉)
Department of Nuclear Medicine, Korea Cancer
Center Hospital, 215-4, Gongneung-dong, Nowon-gu,
Seoul 139-706, South Korea
e-mail: smlim328@kcch.re.kr

J.-S. Koh
Department of Pathology, Korea Cancer
Center Hospital, Seoul, South Korea

J. Y. Yoo
Department of Radiology, Korea Cancer
Center Hospital, Seoul, South Korea

Introduction

Osteosarcoma is the most common pediatric malignant bone tumor with an incidence of only a few cases per million person-years on a worldwide basis [1]. The inclusion of aggressive polychemotherapy and the interdisciplinary treatment concept has dramatically improved the long-term survival of patients with osteosarcoma. Response to preoperative chemotherapy has been reported to be the most powerful prognostic indicator of survival in osteosarcoma patients [1, 2].

However, histologic response can only be determined in resected specimens, and thus, response monitoring during the course of chemotherapy is not possible [3, 4]. To overcome these limitations, other diverse imaging modalities have been investigated [5].

PET using [^{18}F]FDG can detect changes in tissue metabolism that usually precede structural changes [6], and several studies have shown that FDG PET is useful for noninvasive evaluation of response to neoadjuvant chemotherapy in osteosarcoma [5, 7–11]. Of the various parameters used for measuring tumor glucose metabolic activity, maximum standardized uptake value (SUV_{max}) provides the most robust measurement in sarcoma [12]. However, the correlation between SUV_{max} values, which represent only a pixel-sized region of interest (ROI), and histologic response, which averages the percentage tumor necrosis across the entire resected tumor specimen, is not fully understood [8, 13].

In this prospective study, we evaluated the usefulness of SUV_{max} in predicting and assessing histologic response to neoadjuvant chemotherapy in patients with osteosarcoma. We also analyzed the correlation between FDG PET imaging findings and response to chemotherapy in osteosarcoma using parallel PET and MRI.

Materials and methods

Patient selection

A total of 26 consecutive patients with osteosarcoma treated at our institution were prospectively enrolled between May 2010 and August 2011. Eligibility requirements included biopsy-proven primary high-grade extremity osteosarcoma, the completion of neoadjuvant chemotherapy and surgery, FDG PET/CT and MRI scans obtained before and after neoadjuvant chemotherapy, a time between the first FDG PET scan and the initiation of chemotherapy of no more than 2 weeks, and a time between the second FDG PET scan and surgery of no more than 2 weeks.

All patients underwent a conventional evaluation (plain radiography and MRI of the primary tumor, a $^{99\text{m}}\text{Tc}$ -methylene diphosphonate bone scan, and a CT scan of the chest) and FDG PET before neoadjuvant chemotherapy. Diagnoses were confirmed based on histologic examinations of tumor tissues obtained by open or needle biopsy, which were performed on average 2 days (range 1–5 days) before the first PET scan.

Our institutional review board approved the study. All patients provided written informed consent, and the study was performed according to the ethical guidelines of our institutional clinical research committee.

Installation and imaging protocol of parallel PET/MRI

A whole-body FDG PET/CT scanner (Biograph6; Siemens Medical Solutions, Malvern, PA) and a 3.0-T whole-body MRI scanner (MAGNETOM Trio A Tim; Siemens Medical Solutions, Erlangen, Germany) were installed in parallel. The two scanners were located 10 m apart separated by an antimagnetic wall. The intravenous administration of FDG was followed by a tracer uptake phase of 60 min. FDG PET/CT scans were obtained 60 min after FDG injection and MRI images were acquired 90 min after FDG injection. Both PET/CT and MRI images were acquired in a supine position, and all patients walked from the PET/CT scanner to the MRI scanner (on independent patient tables). FDG PET and MRI images were coregistered using syngo Fused-Vision3D software (Siemens Medical Solutions, Erlangen, Germany).

FDG PET/CT

Patients fasted for at least 6 h before intravenous injection of FDG (8.14 MBq/kg). Truncal PET scans were obtained in two-dimensional mode using five to seven bed positions to ensure adequate coverage from the head to the pelvic floor. Additional regional PET scans were also acquired in the same manner as the truncal scans (using three to five bed positions) to cover tumor sites located in the lower extremities. The CT scans were obtained immediately before the PET scans using a six-slice helical CT scanner. The imaging parameters used were as follows: 130 kVp, 30 mA, 0.6 s/CT rotation, and a pitch of 6. No contrast material was administered. Additional PET/CT scans (six or seven bed positions) were acquired in the same manner as the whole-body scans to cover tumor sites located in the extremities. Emission data were acquired for 3.5 min for each bed position. PET/CT images were reconstructed using the ordered-subsets expectation maximization algorithm (two iterations, eight subsets) with CT-based attenuation correction, after rebinning three-dimensional sinogram using Fourier Rebinning, and smoothed using a 5-mm post-gaussian filter.

FDG PET/CT image interpretation

Abnormal FDG uptake was defined as FDG uptake greater than that in adjacent normal bone. Areas of abnormal FDG uptake were identified, and intensities of FDG uptake were quantified by calculating SUVs from the amounts of FDG injected, total body weight, and regional uptake in attenuation-corrected regional images. Specifically, SUV was defined as the SUV_{max} of the ROI and calculated from the following equation: (activity/unit volume)/(injected dose/total body weight). PET data were interpreted by an experienced nuclear physician.

MRI

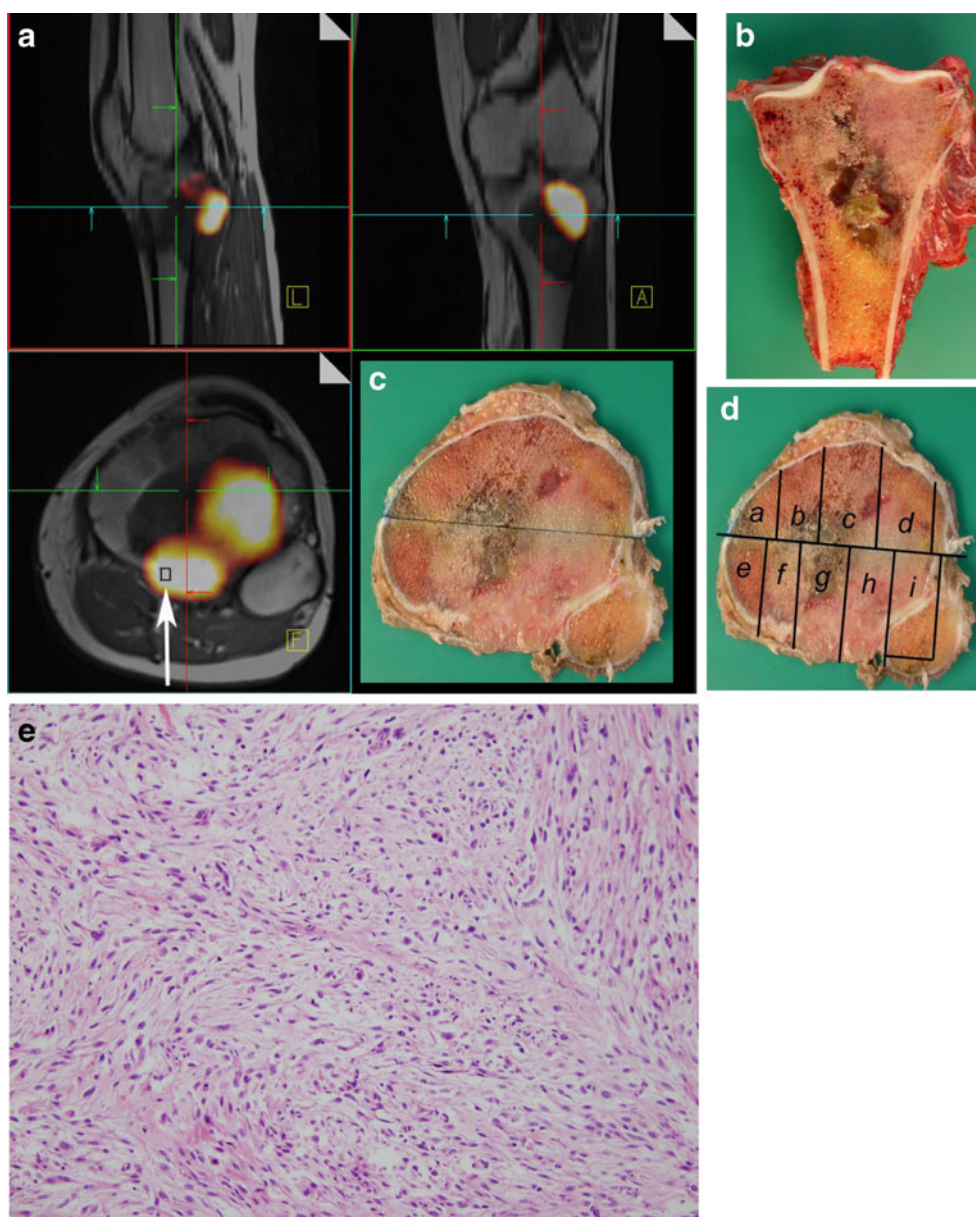
MR images were obtained using a body array surface coil. To ensure the patient's limbs were in an identical position for PET and MRI, an in-house designed positioning device was used. MRI sequences included a standard T1-weighted sequence (TR/TE 752/10 ms; field of view 450 mm, matrix size 279 × 448; slice thickness 5 mm; 2 average; acquisition time 3 min 53 s), with or without gadolinium enhancement, and a T2-weighted sequence (TR/TE 3,360/97 ms; field of view 450 mm, matrix size 298 × 448; slice thickness 5 mm; 2 average; acquisition time 3 min 7 s), without fat suppression. Gadodiamide (Omniscan; GE Healthcare) was administered intravenously. Intramedullary tumor lengths were measured on coronal sections of unenhanced T1-weighted sequences,

and tumor widths and depths were measured on enhanced axial T1-weighted sequences without fat suppression [14]. MR images were independently reviewed by two of the authors. When these two reviewers found a size discrepancy of more than 10 %, images were reviewed simultaneously. Decisions were made in consensus.

Neoadjuvant chemotherapy

All patients underwent two cycles of preoperative chemotherapy using the modified T10 protocol [15]. Briefly, each chemotherapy cycle consisted of high-dose methotrexate, Adriamycin, and cisplatin. Methotrexate at a dose of 8 to 12 g/m² was administered twice, on days 1 and 7. On day 14, cisplatin was administered at 100 mg/m² over 2 h.

Fig. 1 A PET/MRI image was used to locate the point of maximum metabolic activity (SUVmax) in the resected specimen. **a** The physical location of SUVmax was determined using standard imaging software (*arrow*). **b** The resected specimen was initially cut longitudinally in the mid-coronal plane. **c** Using the premeasured distance from the joint line (determined using a PET/MRI image), the specimen was cut axially. This gross axial section corresponds to a plane containing the SUVmax. **d** Pathologic mapping was used to locate the point of maximum metabolic activity (SUVmax). The tissue section labeled **g** contains the highest metabolic activity point in the tumor. **e** Hematoxylin and eosin staining of the area corresponding to the SUVmax location shows no effect of chemotherapy, which means that the minimum histologic response in this patient was 0 %. The percentage necrosis on histology of the entire resected specimen was 60 % (**e** ×200)



Subsequently, Adriamycin was administered at 60 mg/m² for 18 h. The intervals between the end of the first cycle of chemotherapy and initiation of the second cycle, and between the end of the second cycle and surgery, were around 3 weeks.

Histologic assessments using PET/MRI images

For detailed specimen mapping, samples were sectioned by an experienced pathologist and an orthopedic surgeon in concert. SUVmax represents the volume of greatest metabolic activity in a tumor, and the physical location of this volume can be ascertained using standard imaging software [13]. In the present study, to locate SUVmax in resected specimens, we applied a technique called mapping. First, the voxel with the SUVmax was selected by adjusting the window of the PET image on the coregistered PET/MRI image. Second, the coronal MRI slice containing the SUVmax was selected and the distance (*Z*) from the pixel with the SUVmax to the articular surface was measured. Third, the axial MRI slice with the SUVmax was selected and the horizontal and vertical distances (*X* and *Y*, respectively) from the pixel with the SUVmax to the axis of long bone were measured. Fourth, one coronal plane *Y* mm (anterior or posterior) from the axis of the long bone was selected from among initially cut coronal planes with a thickness of 4 mm. Fifth, on this coronal plane, one transaxial plane *Z* mm from the articular surface was cut at a thickness of 3 mm. Finally, from this stick-like specimen, a 4×4×3-mm specimen *X* mm from the axis of the long bone was cut and analyzed (Fig. 1) [13, 16]. Using this method, we were able to determine percentage necrosis by histology at the highest metabolic activity point in a tumor as determined by FDG PET. Because the volume of interest of the SUVmax area was 4×4×3 mm, we determined a 4×4-mm ROI in the corresponding pathologic specimen. This was defined as the minimum histologic response, which can be considered as the percentage necrosis in the region corresponding to SUVmax.

Histologic responses to preoperative chemotherapy were graded using tumor necrosis percentages as grade III and IV (necrosis of 90 % or more), indicating a good response, and grades I and II (less than 90 % necrosis), indicating a poor response [4, 16].

Definition and calculation of parameters

We defined prechemotherapy SUVmax as SUV1 and preoperative SUVmax as SUV2. The SUV change ratio (SCR) was defined as the ratio SUV2 to SUV1. Tumor volumes were determined using MR images as described by [17]

using the ellipsoid formula: tumor volume=0.53 × tumor length × tumor width × tumor depth [14, 18].

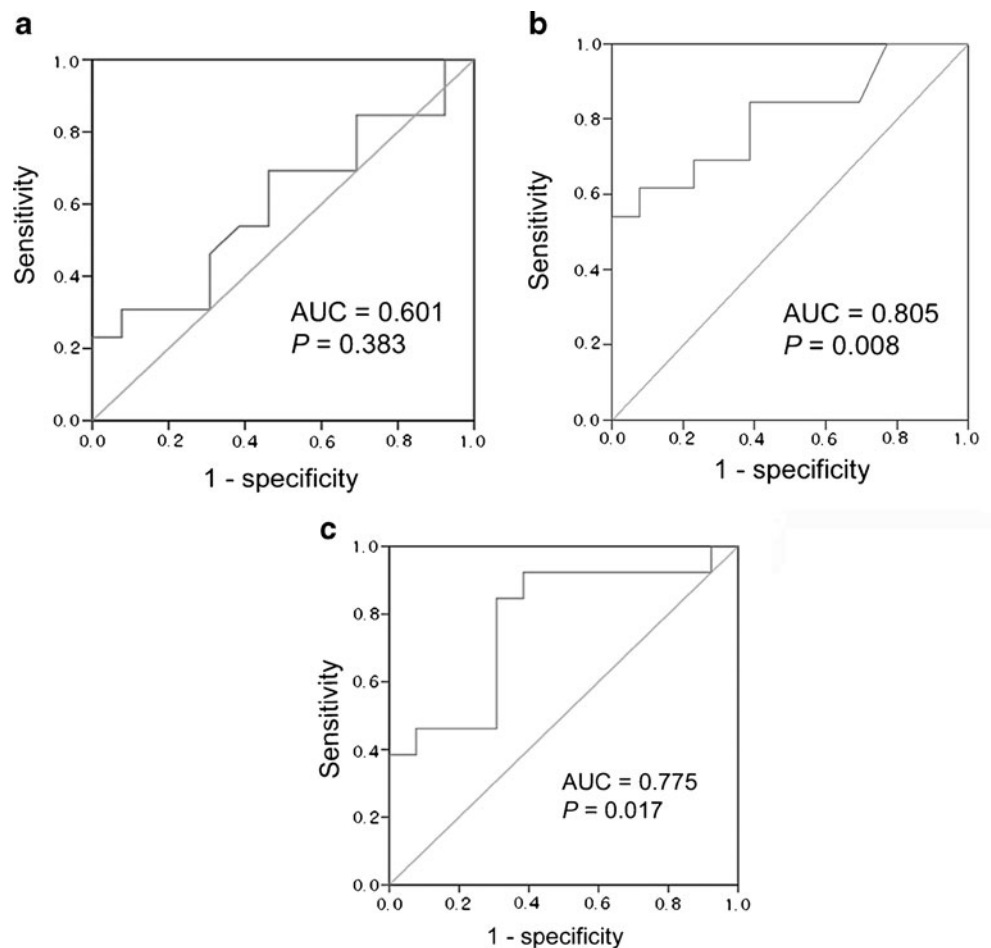
Statistics

We analyzed SUV1, SUV2 and SCR in terms of their ability to discriminate responders from nonresponders. For this purpose, we plotted receiver operating characteristic

Table 1 Patient characteristics

Characteristics	Value
Age (years), <i>n</i> (%)	
≤15	13 (50.0)
>15 to ≤40	10 (38.5)
>40	3 (11.5)
Gender, <i>n</i> (%)	
Male	16 (61.5)
Female	10 (38.5)
AJCC stage, <i>n</i> (%)	
IIA	14 (53.8)
IIB	8 (30.8)
III	1 (3.8)
IV	3 (11.6)
Tumor volume (cm ³), mean (range)	128 (20–407)
Tumor volume (cm ³), <i>n</i> (%)	
≤150	18 (69.2)
>150	8 (30.8)
Location, <i>n</i> (%)	
Distal femur	13 (50.1)
Proximal tibia	9 (34.6)
Proximal femur	2 (7.7)
Other	2 (7.7)
SUV1, mean (range)	9.2 (2.9–31.2)
SUV2, mean (range)	5.3 (1.5–15.7)
Time from first PET to initiation of chemotherapy (days), mean (range)	3 (1–6)
Time from second PET to surgery (days), mean (range)	3 (1–13)
Pathologic subtype, <i>n</i> (%)	
Osteoblastic	21 (80.8)
Chondroblastic	1 (3.8)
Fibroblastic	3 (11.6)
Other	1 (3.8)
Operation type, <i>n</i> (%)	
Amputation	0 (0)
Limb salvage	26 (100)
Histologic response, <i>n</i> (%)	
Good	13 (50.0)
Poor	13 (50.0)
Total	26 (100)

Fig. 2 ROC curves of SUV1 (a), SUV2 (b), and SCR (c) were plotted to predict histologic response. SUV2 and SCR were found to predict histologic response



(ROC) curves and calculated areas under the curve (AUCs) for each parameter. We chose parameters that best predicted response and determined cut-off values that showed the highest accuracies. Spearman's rank correlation test was used to explore correlations between SUV2, minimum histologic response, and histologic response. Analyses were performed using SPSS version 13.0 (SPSS, Chicago, IL). All *P* values were derived from a two-sided test, and values less than 0.05 were considered significant.

Results

Patient characteristics

Patient characteristics are presented in Table 1. The mean age of the patients was 21 years (range 9–55 years), and 61.5 % were male. The average tumor volume was 128 cm³ (range 20–407 cm³). On the basis of the revised American Joint Committee on Cancer staging system [19], 14 patients (53.8 %) had a stage

Table 2 Predictive values of SUV2 and SCR in 26 patients

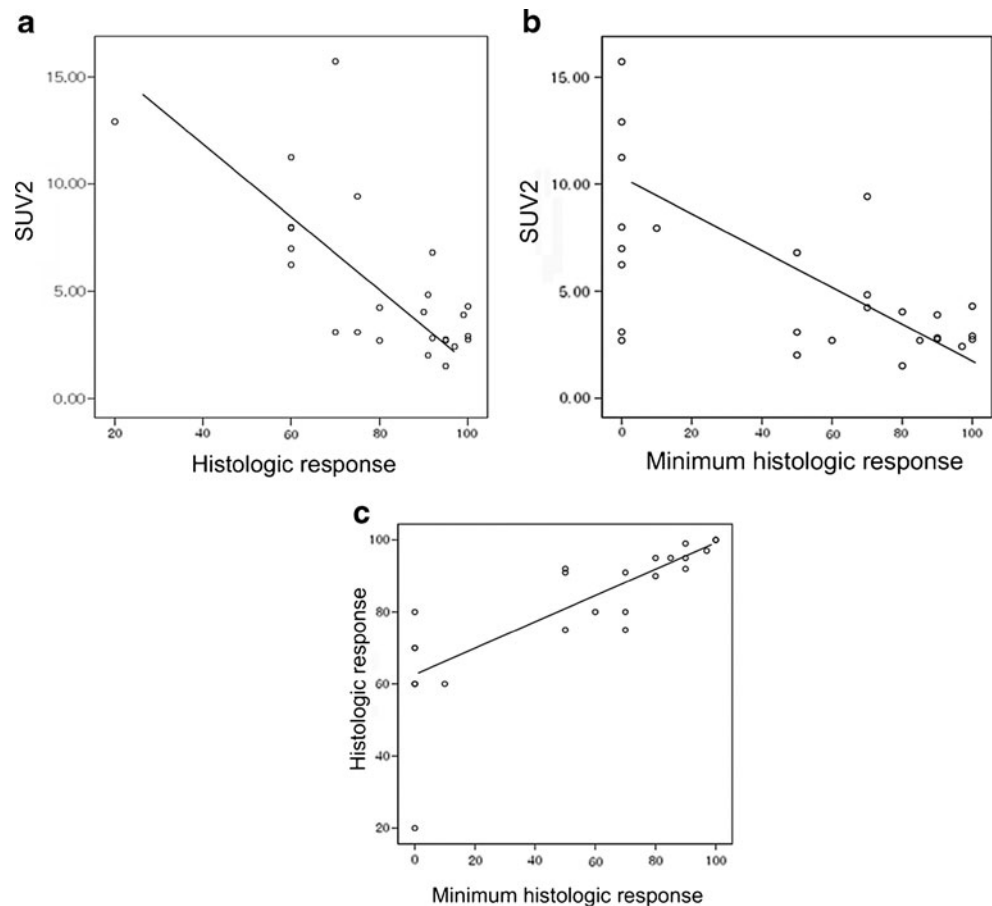
Parameter	Cut-off	No. of patients	No. of poor responders	Sensitivity (%)	Specificity (%)	Positive predictive value (%)	Negative predictive value (%)	Accuracy (%)
SUV2	>4	13	9	69.2	69.2	69.2	69.2	69.2
	>5	9	8	61.5	92.3	88.9	70.6	76.9
	>6.5	8	7	53.8	92.3	87.5	66.7	73.1
SCR	> 0.4	20	12	92.3	38.5	60.0	83.3	65.4
	> 0.5	15	11	84.6	69.2	73.3	81.8	76.9
	> 0.6	10	6	46.2	69.2	60.0	56.3	57.7

IIA tumor, 8 (30.8 %) had a stage IIB tumor, 1 (3.8 %) had a stage III tumor, and 3 (11.6 %) had a stage IV tumor. Half of the 26 patients presented with a tumor in the distal femur. The median time between the first PET examination and the initiation of chemotherapy was 3 days and the median time between the second PET examination and surgery was 3 days. All patients underwent limb salvage surgery and in 13 patients (50.0 %) the resected specimens showed a good histologic response to neoadjuvant chemotherapy.

ROC curve analysis of response prediction

ROC curves of SUV1, SUV2, and SCR were plotted to predict histologic response. SUV2 and SCR predicted histologic response and the AUCs were 0.805 and 0.775, respectively (Fig. 2). A SUV2 cut-off of >5 predicted poor responders with a sensitivity of 61.5 %, a specificity of 92.3 %, a positive predictive value of 88.9 %, and a negative predictive value of 70.6 %. A SCR cut-off of >0.5 predicted poor responders with a sensitivity of 84.6 %, a specificity of 69.2 %, a positive predictive value of 73.3 %, and a negative predictive value of 81.8 % (Table 2).

Fig. 3 Statistically significant correlations were found between SUV2, minimum histologic response, and histologic response. **a** SUV2 was correlated with histologic response (Spearman's rho correlation coefficient -0.642 , $P<0.001$). **b** SUV2 was correlated with minimum histologic response (Spearman's rho correlation coefficient -0.515 , $P=0.007$). **c** Histologic response was correlated with minimum histologic response (Spearman's rho correlation coefficient 0.911 , $P<0.001$)



Correlation among SUV2, minimum histologic response and histologic response

A significant correlation was observed between SUV2 and histologic response (Spearman's rho correlation coefficient -0.642 , $P<0.001$; Fig. 3a), and both SUV2 and histologic response were significantly correlated with minimum histologic response, as illustrated in Fig. 3b and c, respectively (Spearman's rho correlation coefficient -0.515 and 0.911 , $P=0.007$ and $P<0.001$, respectively).

Discussion

FDG PET can detect changes in tissue metabolism that usually precede structural changes, and thus it should be more accurate for assessing treatment response because it can more correctly identify viable residual tumor [5]. Several studies have shown a strong correlation between reductions in tumor glucose metabolism after neoadjuvant chemotherapy and histologic responses of primary bone tumors [5, 7, 8, 20, 21]. For quantification of tumor glucose metabolism, a variety of methods for SUV measurement

Table 3 Previous studies that used SUVmax for predicting response

Reference	No. of patients	Good responders	Poor responders	SUV1	SUV2	Cut-off	Positive predictive value (%)	Negative predictive value (%)
[8]	18	5	13	Mean 8.2 (range 2.5–24.1)	Mean 3.3 (range 1.6–12.8)	SUV2 <2 for good response (<i>n</i> =4)	75	85.7
[21]	10	2	8	Mean 8.2 (range 1.4–13.6)	Mean 4.4 (range 1.7–9.6)	SUV2/SUV1 <0.4 for good response (<i>n</i> =2)	100	100
[5]	70	33	37	Median 8.0 (range 2.4–47.5)	Median 4.5 (range 1.5–16.6)	Algorithm for good response (<i>n</i> =32)	97	95
[11]	31	10	21	Mean 6.3 (range 2.3–15.7)	Mean 3.5 (range 0.7–9.5)	SUV2/SUV1 <0.48 for good response (<i>n</i> =7)	53.8	83.3
Present study	26	13	13	Mean 9.2 (range 2.9–31.2)	Mean 5.3 (range 1.5–15.7)	SUV2 >5 for poor response (<i>n</i> =8)	88.9	70.6

have been used: SUVmax in a single pixel, background-corrected values, larger or smaller ROIs, and total lesion glycolysis [22]. Among them, SUVmax in a single pixel which represents the most aggressive portion is most widely used for determining tumor SUV [23]. As a single-pixel value, however, SUVmax is adversely affected by noise. The peak SUV, defined as the average SUV within a small ROI centered on a high-uptake part of the tumor, has been suggested as a more robust alternative [22]. However, quantification of individual tumor response using peak SUV is highly sensitive to the shape, size, and location of the ROI [24]. Hence SUVmax instead of peak SUV was chosen as the metabolic parameter for assessing histologic response in the current study. Moreover, SUVmax measurements in a single pixel are readily reproducible by drawing a volume of interest that includes the entire tumor [25]. Of the various ROIs that are used to measure SUV, SUVmax is being increasingly used in a wide range of human cancers [22, 26–30]. However, for determining the ROI, it is still unclear whether total tumor volume or the maximum metabolically active portion is more important [22].

In the present preliminary study, we evaluated the potential of FDG PET SUVmax as an early predictor of osteosarcoma response to preoperative chemotherapy. In osteosarcoma, previous studies have used two FDG PET scan parameters, namely tumor-to-background ratio (TBR) and SUVmax. Whereas SUVmax represents the point of highest metabolic activity in a tumor, the TBR represents a semiquantitative index of tumor glucose use. In a previous study in sarcoma patients, TBR demonstrated a significantly higher interobserver variability than SUVmax [12], and therefore, we used SUVmax rather than TBR. Furthermore, in four previous studies that used SUVmax for predicting response, it was found that SUV2/SUV1 and SUV2 were correlated with histologic response (Table 3).

Previous studies have demonstrated a significant association between SUVmax and tumor necrosis [5, 8, 11, 21], which appears a reasonable result because tumor necrosis is the strongest known prognostic factors and high SUVmax values have been shown to correspond to poor survival in osteosarcoma [25, 31]. However, tumor necrosis and FDG PET assessments are quite different. Although these methods evaluate similar biologic features (residual tumor cells after therapy), tumor necrosis is the result of an averaged assessment in a representative plane, whereas FDG PET assessments are based on three-dimensional assessment of maximal remaining tumor activity measured in terms of FDG uptake [31]. Moreover, the location of the SUVmax region cannot always be included during posttherapy histopathologic evaluations of bone specimens [13]. Accordingly, the correlation between SUVmax values and chemotherapy responses in osteosarcoma remains to be validated.

In this preliminary study, we introduced minimum histologic response as an intervening variable to investigate how SUVmax values are correlated with tumor necrosis in osteosarcoma. The locations which represent the point of greatest metabolic activity in tumors can be determined in PET/MRI images using standard imaging software. Since osteosarcoma is a malignancy of bone, its anatomic features can be retained using a technique called mapping [13], which allows the anatomic locations of all submitted tissues to be determined. Thus, we were able to determine the percentage necrosis by histology at the point of greatest metabolic activity in resected specimens (Fig. 1).

One important finding of our study was that more than half of good responders (7/13) showed a good response (≥ 90 % tumor necrosis) at SUVmax locations (Fig. 3c). In particular, three patients with a totally necrotic tumor in whole specimens showed no tumor cells that appeared viable histologically even at SUVmax locations. This may have been because FDG metabolism also reflects a nonspecific (but bioenergetically intense) inflammatory response and scarring around necrotic tumor [8, 31]. On the other hand, eight poor responders showed no effect of chemotherapy at SUVmax locations. These results imply that response prediction using SUVmax cut-off value provides a useful means of predicting poor responders. In the current study, a SUV2 cut-off of >5 showed relatively poor sensitivity (62 %) in spite of good specificity (92 %) for the prediction of a good histologic response. Therefore, another parameter, such as the combined metabolic/volume index, in combination with SUV2 would be helpful [5, 32].

The present study had several inherent limitations. First, the relationship between SUVmax locations and positions in tissue sections was prone to measurement error. Because this method was a highly educated estimate, we determined the physical location of the greatest metabolic activity in the section with a consensus among nuclear physicians, orthopedic surgeons and pathologists. Second, the degree of inflammation or other active processes which also affect SUVmax was not measured. Third, due to the small number of patients, the potential clinical utility of the SUV2 threshold of 5 for distinguishing treatment responders from non-responders may be somewhat overstated. Fourth, our suggested SUV cut-off values may differ for different PET scanners.

Conclusion

In summary, a SUVmax of more than 5 after neoadjuvant chemotherapy identified the majority of histologic nonresponders (sensitivity 61.3 %, positive predictive value 88.9 %). In addition, a significant correlation was found between SUVmax and necrosis percentages determined by

histology at points of greatest metabolic activity, and tumor necrosis at points of maximum metabolic activity were found to be significantly correlated with histologic response in whole resected specimens.

Acknowledgment This study was supported by a grant of the RTR (Radiological Translational Research program), Korea Institute of Radiological & Medical Sciences (50453–2011).

Conflicts of interest None.

References

- Bielack SS, Kempf-Bielack B, Delling G, Exner GU, Flege S, Helmke K, et al. Prognostic factors in high-grade osteosarcoma of the extremities or trunk: an analysis of 1,702 patients treated on neoadjuvant cooperative osteosarcoma study group protocols. *J Clin Oncol*. 2002;20:776–90.
- Kim MS, Lee SY, Lee TR, Cho WH, Song WS, Koh JS, et al. Prognostic nomogram for predicting the 5-year probability of developing metastasis after neo-adjuvant chemotherapy and definitive surgery for AJCC stage II extremity osteosarcoma. *Ann Oncol*. 2009;20:955–60.
- Rosen G, Marcove RC, Caparros B, Nirenberg A, Kosloff C, Huvos AG. Primary osteogenic sarcoma: the rationale for preoperative chemotherapy and delayed surgery. *Cancer*. 1979;43:2163–77.
- Rosen G, Caparros B, Huvos AG, Kosloff C, Nirenberg A, Cacavio A, et al. Preoperative chemotherapy for osteogenic sarcoma: selection of postoperative adjuvant chemotherapy based on the response of the primary tumor to preoperative chemotherapy. *Cancer*. 1982;49:1221–30.
- Cheon GJ, Kim MS, Lee JA, Lee SY, Cho WH, Song WS, et al. Prediction model of chemotherapy response in osteosarcoma by 18F-FDG PET and MRI. *J Nucl Med*. 2009;50:1435–40.
- Hoh CK, Hawkins RA, Glaspy JA, Dahlbom M, Tse NY, Hoffman EJ, et al. Cancer detection with whole-body PET using 2-[18F]fluoro-2-deoxy-D-glucose. *J Comput Assist Tomogr*. 1993;17:582–9.
- Ye Z, Zhu J, Tian M, Zhang H, Zhan H, Zhao C, et al. Response of osteogenic sarcoma to neoadjuvant therapy: evaluated by 18F-FDG-PET. *Ann Nucl Med*. 2008;22:475–80.
- Hawkins DS, Rajendran JG, Conrad 3rd EU, Bruckner JD, Eary JF. Evaluation of chemotherapy response in pediatric bone sarcomas by [F-18]-fluorodeoxy-D-glucose positron emission tomography. *Cancer*. 2002;94:3277–84.
- Franzius C, Bielack S, Flege S, Sciuk J, Jurgens H, Schober O. Prognostic significance of (18)F-FDG and (99m)Tc-methylene diphosphonate uptake in primary osteosarcoma. *J Nucl Med*. 2002;43:1012–7.
- Schulte M, Brecht-Krauss D, Werner M, Hartwig E, Sarkar MR, Keppler P, et al. Evaluation of neoadjuvant therapy response of osteogenic sarcoma using FDG PET. *J Nucl Med*. 1999;40:1637–43.
- Bajpai J, Kumar R, Sreenivas V, Chand Sharma M, Khan SA, Rastogi S, et al. Prediction of chemotherapy response by PET-CT in osteosarcoma: correlation with histologic necrosis. *J Pediatr Hematol Oncol*. 2011;33:e271–8.
- Benz MR, Evilevitch V, Allen-Auerbach MS, Eilber FC, Phelps ME, Czernin J, et al. Treatment monitoring by 18F-FDG PET/CT in patients with sarcomas: interobserver

- variability of quantitative parameters in treatment-induced changes in histopathologically responding and nonresponding tumors. *J Nucl Med.* 2008;49:1038–46.
13. Costelloe CM, Raymond AK, Fitzgerald NE, Mawlawi OR, Nunez RF, Madewell JE, et al. Tumor necrosis in osteosarcoma: inclusion of the point of greatest metabolic activity from F-18 FDG PET/CT in the histopathologic analysis. *Skeletal Radiol.* 2010;39:131–40.
 14. Kim MS, Lee SY, Cho WH, Song WS, Koh JS, Lee JA, et al. Tumor necrosis rate adjusted by tumor volume change is a better predictor of survival of localized osteosarcoma patients. *Ann Surg Oncol.* 2008;15:906–14.
 15. Rosen G, Marcove RC, Huvos AG, Caparros BI, Lane JM, Nirenberg A, et al. Primary osteogenic sarcoma: eight-year experience with adjuvant chemotherapy. *J Cancer Res Clin Oncol.* 1983;106 Suppl:55–67.
 16. Coffin CM, Lowichik A, Zhou H. Treatment effects in pediatric soft tissue and bone tumors: practical considerations for the pathologist. *Am J Clin Pathol.* 2005;123:75–90.
 17. Göbel V, Jürgens H, Etspüler G, Kemperdick H, Jungblut RM, Stienen U, et al. Prognostic significance of tumor volume in localized Ewing's sarcoma of bone in children and adolescents. *J Cancer Res Clin Oncol.* 1987;113:187–91.
 18. Bieling P, Rehan N, Winkler P, Helmke K, Maas R, Fuchs N, et al. Tumor size and prognosis in aggressively treated osteosarcoma. *J Clin Oncol.* 1996;14:848–58.
 19. Kim MS, Lee SY, Cho WH, Song WS, Koh JS, Lee JA, et al. An examination of the efficacy of the 8 cm maximal tumor diameter cutoff for the subdivision of AJCC stage II osteosarcoma patients. *J Surg Oncol.* 2008;98:427–31.
 20. Franzius C, Sciuk J, Brinkschmidt C, Jurgens H, Schober O. Evaluation of chemotherapy response in primary bone tumors with F-18 FDG positron emission tomography compared with histologically assessed tumor necrosis. *Clin Nucl Med.* 2000;25:874–81.
 21. Huang TL, Liu RS, Chen TH, Chen WY, Hsu HC, Hsu YC. Comparison between F-18-FDG positron emission tomography and histology for the assessment of tumor necrosis rates in primary osteosarcoma. *J Chin Med Assoc.* 2006;69:372–6.
 22. Wahl RL, Jacene H, Kasamon Y, Lodge MA. From RECIST to PERCIST: evolving considerations for PET response criteria in solid tumors. *J Nucl Med.* 2009;50 Suppl 1:122S–50.
 23. Velasquez LM, Boellaard R, Kollia G, Hayes W, Hoekstra OS, Lammertsma AA, et al. Repeatability of 18F-FDG PET in a multicenter phase I study of patients with advanced gastrointestinal malignancies. *J Nucl Med.* 2009;50:1646–54.
 24. Vanderhoek M, Perlman SB, Jeraj R. Impact of the definition of peak standardized uptake value on quantification of treatment response. *J Nucl Med.* 2012;53:4–11.
 25. Costelloe CM, Macapinlac HA, Madewell JE, Fitzgerald NE, Mawlawi OR, Rohren EM, et al. 18F-FDG PET/CT as an indicator of progression-free and overall survival in osteosarcoma. *J Nucl Med.* 2009;50:340–7.
 26. Martoni AA, Zamagni C, Quercia S, Rosati M, Cacciari N, Bernardi A, et al. Early (18)F-2-fluoro-2-deoxy-d-glucose positron emission tomography may identify a subset of patients with estrogen receptor-positive breast cancer who will not respond optimally to preoperative chemotherapy. *Cancer.* 2010;116:805–13.
 27. Kumar A, Kumar R, Seenu V, Gupta SD, Chawla M, Malhotra A, et al. The role of 18F-FDG PET/CT in evaluation of early response to neoadjuvant chemotherapy in patients with locally advanced breast cancer. *Eur Radiol.* 2009;19:1347–57.
 28. Lee HY, Lee HJ, Kim YT, Kang CH, Jang BG, Chung DH, et al. Value of combined interpretation of computed tomography response and positron emission tomography response for prediction of prognosis after neoadjuvant chemotherapy in non-small cell lung cancer. *J Thorac Oncol.* 2010;5:497–503.
 29. Guerra L, Niespolo R, Di Pisa G, Ippolito D, De Ponti E, Terrevazzi S, et al. Change in glucose metabolism measured by 18F-FDG PET/CT as a predictor of histopathologic response to neoadjuvant treatment in rectal cancer. *Abdom Imaging.* 2011;36:38–45.
 30. Chung HW, Lee EJ, Cho YH, Yoon SY, So Y, Kim SY, et al. High FDG uptake in PET/CT predicts worse prognosis in patients with metastatic gastric adenocarcinoma. *J Cancer Res Clin Oncol.* 2010;136:1929–35.
 31. Hawkins DS, Conrad 3rd EU, Butrynski JE, Schuetz SM, Eary JF. [F-18]-fluorodeoxy-D-glucose-positron emission tomography response is associated with outcome for extremity osteosarcoma in children and young adults. *Cancer.* 2009;115:3519–25.
 32. Im HJ, Kim TS, Park SY, Min HS, Kim JH, Kang HG, et al. Prediction of tumour necrosis fractions using metabolic and volumetric 18F-FDG PET/CT indices, after one course and at the completion of neoadjuvant chemotherapy, in children and young adults with osteosarcoma. *Eur J Nucl Med Mol Imaging.* 2012;39:39–49.